



A multi-reference poly-conformational method for *in silico* design, optimization, and repositioning of pharmaceutical compounds illustrated for selected SARS-CoV-2 ligands

Vadim Alexandrov¹, Alexander Kirpich², Omar Kantidze³ and Yuriy Gankin³

¹Liquid Algo LLC, Hopewell Junction, NY, United States of America

²Department of Population Health Sciences, School of Public Health, Georgia State University, Atlanta, GA, United States of America

³Quantori, Cambridge, MA, United States of America

ABSTRACT

Background. This work presents a novel computational multi-reference poly-conformational algorithm for design, optimization, and repositioning of pharmaceutical compounds.

Methods. The algorithm searches for candidates by comparing similarities between conformers of the same compound and identifies target compounds, whose conformers are collectively close to the conformers of each compound in the reference set. Reference compounds may possess highly variable MoAs, which directly, and simultaneously, shape the properties of target candidate compounds.

Results. The algorithm functionality has been case study validated *in silico*, by scoring ChEMBL drugs against FDA-approved reference compounds that either have the highest predicted binding affinity to our chosen SARS-CoV-2 targets or are confirmed to be inhibiting such targets *in-vivo*. All our top scoring ChEMBL compounds also turned out to be either high-affinity ligands to the chosen targets (as confirmed in separate studies) or show significant efficacy, *in-vivo*, against those selected targets. In addition to method case study validation, *in silico* search for new compounds within two virtual libraries from the Enamine database is presented. The library's virtual compounds have been compared to the same set of reference drugs that we used for case study validation: Olaparib, Tadalafil, Ergotamine and Remdesivir. The large reference set of four potential SARS-CoV-2 compounds has been selected, since no drug has been identified to be 100% effective against the virus so far, possibly because each candidate drug was targeting only one, particular MoA. The goal here was to introduce a new methodology for identifying potential candidate(s) that cover multiple MoA-s presented within a set of reference compounds.

Submitted 28 March 2022

Accepted 26 September 2022

Published 24 November 2022

Corresponding author

Yuriy Gankin,
yuriy.gankin@quantori.com

Academic editor

Marisa Nicolás

Additional Information and
Declarations can be found on
page 15

DOI 10.7717/peerj.14252

© Copyright
2022 Alexandrov et al.

Distributed under
Creative Commons CC-BY 4.0

OPEN ACCESS

Subjects Biochemistry, Drugs and Devices, Infectious Diseases, Data Mining and Machine Learning, COVID-19

Keywords Conformers, Multi-reference, Poly-conformational, SARSCOV- 2, *In silico*, Ligand-based, Structure-based, Virtual library, Computational framework, Validation

INTRODUCTION

Most of the small molecules exist in multiple conformations (shapes) based on their surrounding environmental conditions. Each 3D shape of a molecule enables it to fit into the binding pockets of proteins and dictates its biological activity. Often, distinctly different chemical compounds that have similar shapes and similar charge distributions along the molecular surface can bind the same target. Therefore, it is beneficial to compare shapes and surface distribution charges for target query and reference compounds on a conformer-by-conformer basis. If one of the conformers of the query molecule matches one of the conformers (especially bound-to-target) of the reference molecule, there is a chance that the reference compound will also exhibit similar binding properties to the same target.

OpenEye Scientific Software Inc. pioneered an algorithm and the corresponding tool, Rapid Overlay of Chemical Structures (ROCS) ([Grant, Gallardo & Pickup, 1996](#); [OpenEye Scientific Software, Inc., 2008](#)) for comparing shapes of molecules by overlaying and measuring their molecular structures *in silico* and comparing differences between a query and reference molecule. ROCS performs a shape-based overlay of a query conformer to a potential hit molecule by utilizing Gaussian atom-centered functions. The overlap is then expressed as a normalized value ranging between “0” and “1”, where “0” means no overlay and “1” means the maximum possible overlay. Atomic charges on the surface of the molecule are accounted for by using a separate score called “color”, so ROCS algorithm attempts to maximize both shape and “color” overlay. The “color” score also ranges from “0” to “1”, where “0” means no “color” similarity and “1” means a perfect color overlay. The final score thus ranges from 0 to 2. Thus, ROCS identifies potentially active compounds by comparing their shapes via *explicit alignment*; it is competitive and often superior to structure-based approaches in virtual screening ([Hawkins, Skillman & Nicholls, 2007](#); [Venhorst et al., 2008](#)) both in terms of overall performance and consistency ([Sheridan, McGaughey & Cornell, 2008](#)). As a result, novel molecular scaffolds have been identified by using ROCS against various targets which have been considered very difficult to address computationally ([Kumar et al., 2014](#); [Kumar et al., 2016](#); [Chen et al., 2018](#); [Khan et al., 2019](#); [Rush 3rd et al., 2005](#)).

Being a computationally-intensive process, the overlapping of molecular shapes represents a bottleneck in the search for similar molecules. This remains despite the recent so-called PAPER implementation of ROCS on GPU ([Haque & Pande, 2010](#)) and the development of FastROCS ([OpenEye Scientific Software, Inc, 2011](#)) for large (>1B) compound libraries. Alternative methods perform overlaying by comparing shape-based descriptors *without* performing explicit shape alignment, specifically conformer-level 3D fingerprints. An example of such an approach is ElectroShape, implemented in the the Open Drug Discovery Toolkit (ODDT) package ([Wójcikowski et al., 2019](#)) which uses an algorithm incorporating shape, chirality, and electrostatics ([Ballester & Richards, 2007b](#); [Armstrong et al., 2010](#)) and represents each conformer via a fixed-length vector of real-valued numbers. Similarly, the Extended 3-Dimensional FingerPrint (E3FP) package ([Axen et al., 2017](#)) also utilizes an *alignment-invariant* 3D representation of molecular conformers

as a fixed-length binary vector for each conformer. These fingerprint-based approaches allow for the similarity calculation between two molecular shapes either as a Tanimoto distance (for binary fingerprints) or Euclidean distance (for real-valued fingerprints) computations. Such computations are orders of magnitude faster in comparison to alternative methods that require the actual alignment of the two compared conformers. The Ultrafast Shape Recognition (USR) method can speed up such virtual screening even more ([Ballester & Richards, 2007a](#)). Although the calculation of a shape-based fingerprint for each conformer can be a rather computationally involved procedure, as soon as all conformers for the virtual library are fingerprinted and stored in a database, the similarity search for the query molecule in such a database is computationally quick. Comparative performance of the two approaches (explicit shapes alignment *vs* shapes' fingerprints comparison) in terms of accuracy (hit enrichment) was exhaustively studied for many virtual screening setups ([Hawkins, Skillman & Nicholls, 2007](#); [Kirchmair et al., 2009](#); [Schreyer & Blundell, 2012](#)) and was found to be comparable.

Here, we present MultiRef3D, a novel computational multi-reference poly-conformational algorithm for the design, optimization, and repositioning of pharmaceutical compounds. The algorithm searches for small molecules by comparing similarities between conformers of the same compound and identifies hits, whose conformers are collectively close to the conformers of each compound in a reference set. Reference compounds may represent well-characterized ligands and possess a highly variable mode of action (MoA). The principal and computationally efficient feasibility of this task is illustrated here by using pharmaceuticals that have been shown *in silico* to bind three different proteins of the SARS-CoV-2 as reference compounds. Although the SARS-CoV-2-induced COVID-19 pandemic is one of the biggest challenges worldwide, the highly effective drug for SARS-CoV-2 treatment has not been developed yet. Thus, the potential identification of the small molecule simultaneously targeting several viral proteins may represent an efficient antiviral drug discovery strategy. Moreover, for such a multi-reference search viruses which are the biological systems strongly dependent on the activity of different proteins may represent more illustrative examples than complex age-associated diseases such as cancer, neurodegeneration, psychiatric disorders, *etc.*

For method case study validation, we used the public ChEMBL (version 28) database ([Gaulton et al., 2011](#)) to screen compounds against the most important viral targets, namely 3C-like protease (3CLpro; Mpro), papain-like protease (PLpro) and RNA-dependent RNA polymerase (RdRp). These targets play a major role in virus replication/transcription and host cell recognition and are, therefore, vital for the viral reproduction and spread of infection. Since the method doesn't directly use target information but rather analyzes 3D shapes for a compound that was already predicted, or has been experimentally found to be effective against a particular target (a reference compound), one has to choose one (or more) such compounds as a reference for each target. The focus for each of the above SARS-CoV-2 targets (3CLpro, PLpro and RdRp) was on the reference compounds with the highest binding affinities from the recent *in silico* multi-target repurposing study ([Murugan et al., 2020](#)). For the new compound search (virtual library screening) we used the same set of reference compounds as we used for the method case study validation.

MATERIALS & METHODS

Representative conformer space and conformer-by-conformer comparison

The proposed computational algorithm extends upon currently available methods ([Ballester & Richards, 2007b](#); [Armstrong et al., 2010](#); [Axen et al., 2017](#); [Wójcikowski et al., 2019](#)) and introduces additional search flexibility via the use of the compound conformers. The proposal is to compare multiple possible shapes, adopted via varying environmental conditions, of the same molecule (*i.e.*, conformers) rather than just a single shape that was used previously. In particular, the suggested approach is based on matching ligand-ligand fingerprints without explicitly using target structure information, in contrast to docking and molecular dynamics approaches that simulate the physical binding of a ligand to the target. The supporting theory behind the method is based on the decision to treat conformers, which might have different binding characteristics and properties, as independent entities. In such an approach, each conformer has the corresponding independent alignment-free, 3D-similarity scoring using known multi-references. All conformers were generated using the Experimental-Torsion basic Knowledge Distance Geometry (ETKDG) algorithm implemented in RDKit ([Wang et al., 2020b](#)). ETKDG builds on the classical Blaney and Dixon's ([Blaney & Scott Dixon, 2007](#)) Distance Geometry (DG) algorithm (sampling from all theoretically possible interatomic distances in a given molecule) by combining knowledge of preferred Torsional angles derived from Experimentally determined crystal structures (ETDG), and by further adding constraints from chemical Knowledge, such as 'aromatic rings are flat', or 'bonds connected to triple bonds are colinear' (ETKDG).

Benchmarking studies have found ETKDG to be the best-performing freely available conformer generator up-to-date ([Friedrich et al., 2017b](#); [Friedrich et al., 2017a](#)) providing diverse and chemically-meaningful conformers reproducing crystal conformations.

Unlike what the majority of computational methods had assumed a couple of decades ago (*e.g.* in the CoMFA method ([Gohda et al., 2000](#))), recent research indicates that the bioactive conformation is not necessarily the lowest-energy conformation in the presence of the receptor ([Hasegawa, Arakawa & Funatsu, 2000](#); [Mackerell Jr, 2004](#); [Acharya et al., 2011](#)). In particular, as long as an increase in energy for less favorable conformation is compensated by its binding to the target, *i.e.* the total ligand-target energy is lower than the sum of the energies for the non-bound target and ligand, the bound state is favored. The proposed method emphasizes and relies on this ligand's ability to use its potentially higher energy conformations, depending on the target it attempts to bind. Note, however, that when a sufficiently large number of conformers is requested, ETKDG algorithm generates more conformers with lower energy than with higher energy ([Friedrich et al., 2017b](#); [Friedrich et al., 2017a](#)), therefore when averaged over all conformers (and we generate 100 conformers per molecule), conformers with the lower energy will contribute more to the total overlap.

One of the things that distinguishes ligand-based 3D virtual screening methods from 2D methods is that one has to start worrying about how many conformers to include in the reference set. If the molecule is flexible, it can assume many shapes and pharmacophores.

How to deal with this is one of the fundamental questions in ligand-based virtual screening (LBVS).

In a recent paper by the Schrödinger team, *Cappel et al. (2014)* performed comprehensive benchmark analysis and found that the number of conformers needed for 3D LBVS is actually relatively low: 100 or less to achieve good performance. Thus, we used ETKDG to generate 100 conformers per molecule in this work compound to make sure that the conformational space is adequately covered. Some query ligands with few rotatable bonds can have many very similar conformers, which would mean that the molecule “spends more time” in such conformational states, which would further mean that if those conformers overlap closely with the reference conformers, the result would be more statistically sound (the contributions of such “overrepresented” conformers would weigh more in the average query-reference overlap score for that query compound, in the spirit of Gibbs sampling (*Geman & Geman, 1984; Seep et al., 2021*), which assigns greater weight to samples that occur more frequently in the sampled distribution).

The authors call the approach MultiRef3D to emphasize that it is a fast, alignment-free multi-objective optimization protocol that maximizes the 3D overlap of a query molecule’s conformational ensemble with conformational ensembles of multiple reference ligands. The diagram of the proposed method is summarized in [Fig. 1](#). The formal details of the approach are discussed further.

Efficiency and a conformer scoring

Fingerprinting of individual conformers for alignment-free comparisons became popular in the past few years (*Wójcikowski, Zielenkiewicz & Siedlecki, 2015; Axen et al., 2017; Gladysz et al., 2018; Wang et al., 2020a*). In our algorithm, each conformation is treated as an independent entity and is characterized by a vector of features (fingerprint) which describes its 3D shape along with the distribution of electrostatic charge (both denoted further as electroshape) across its molecular surface. In this work, we used 15-dimensional USRCAT fingerprints (*Schreyer & Blundell, 2012*) which distil molecular shape into a rotation-invariant descriptor vector made up of 15 real numbers describing distance distribution among atoms, atomic partial charges, and atom types. The USRCAT fingerprints were shown to significantly outperform just shape-based fingerprints in recent benchmark tests (*Schreyer & Blundell, 2012; Bonanno & Ebejer, 2020*). Since USRCAT fingerprints reflect both relative 3D positions for all atom types and molecular surface charges for each query molecule conformer as well as for all conformers of the reference compound, they are very well-suited for alignment-free fast computation of conformer similarity. Each conformer is coded within the algorithm by a single fingerprint represented as a fixed-length vector of numbers which ensures computational efficiency. These fingerprints for each of the query and reference molecule conformers are individually scored by the Euclidean distance, serving as a similarity measure between two conformers. Note that both Euclidean distance and Tanimoto index can serve as similarity measures for these and other real-valued fingerprints (*Bajusz, Rácz & Héberger, 2015*). We chose Euclidean distance as our metric since this choice for the shape-based fingerprints has been already extensively studied and validated, showing superior performance on the DUD dataset (*Armstrong et al., 2010*).

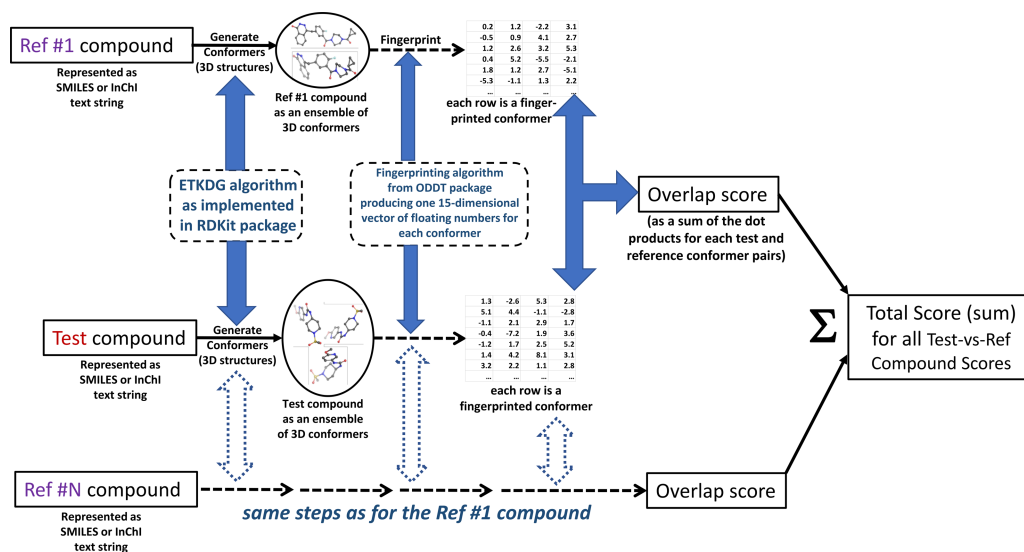


Figure 1 MultiRef3D screening method diagram for multi-conformer and multi-reference screening procedure. For each test compound multiple conformers and the corresponding overlapping scores are computed. Later, the overlapping scores are summed into the total score for the selected test compound. The figure has been created in Microsoft PowerPoint 2016, pyMOL v2.5 (pymol.org) and RDKit v2021.03.01 software (rdkit.org).

Full-size DOI: 10.7717/peerj.14252/fig-1

Objective function optimization

The sum of the conformer-to-conformer similarity scores between the query and reference compound are compared via an objective similarity function W_c for each reference compound c . The goal is to maximize the sum of those individual objective similarity functions across all reference compounds of interest $c = 1, 2, \dots, C$ where c is a summation index for the desired set of reference compounds:

$$W_{All} = \sum_{c=1}^C W_c = \sum_{c=1}^C \sum_{q=1}^Q \sum_{r=1}^R S_{q,r}^{(c)}. \quad (1)$$

In formula Eq. (1) the summand $S_{q,r}^{(c)}$ is the similarity (overlap) of the query conformer q ($q = 1, 2, \dots, Q$) with the conformer r ($r = 1, 2, \dots, R$) for each reference compound c ($c = 1, 2, \dots, C$). For the real-valued fingerprints, the similarity summand between the pair of conformers of interest indexed by query index q and reference index r for compound c is calculated as:

$$S_{q,r}^{(c)} = 1 - (1/N) \sqrt{\sum_{n=1}^N (x_{q,n}^{(c)} - x_{r,n}^{(c)})^2} \quad (2)$$

where $x_{q,n}^{(c)}$ and $x_{r,n}^{(c)}$ are the corresponding normalized fingerprint vector coordinates for $n = 1, 2, \dots, N$. The length (the number of coordinates) of the fingerprint N is determined based on the problem-specific target-ligand interaction characteristics. Since the fingerprint coordinates $x_{q,n}^{(c)}$ and $x_{r,n}^{(c)}$ are normalized (*i.e.* have values between 0 and 1 for each coordinate n) the resulting overlap $S_{q,r}^{(c)}$ is maximized with the value equal to 1, when the fingerprints of both conformers are identical, and can take the smallest value equal to 0, when all

the fingerprint coordinates have a difference equal to 1 *i.e.* as different as possible at the normalized scale.

When the objective is to identify a novel compound for just a single active conformation ($r = 1$) of one ($c = 1$) reference compound (*e.g.* a reference ligand co-crystallized with one particular target) then all conformers for the query molecule are scored against only one active reference conformer. However, in the case when multiple reference compounds are bound to the same target (or sets of reference compounds bound to multiple targets), the total objective function comes into play. It is important to point out that the proposed method is not limited to the structure-based design situations: when several reference compounds are found to be active in a functional assay (and either the target(s) is unknown or the crystal structure of the target is not available)—the formula works just as well (as long as the ligand structure is known). The method becomes especially handy, when there is a great diversity among active reference compounds, whether the target structural information is known or not—the objective function will extract and sum up the similarities for all of the relevant parts of the fingerprinted conformer representations responsible for the observed activity.

The query compound can be evaluated against multiple reference compounds on a conformer-by-conformer basis. In such cases, the corresponding similarity scores are summed and constitute the multi-reference conformer-level objective function to maximize. This can be readily used in a typical ligand-based design setting. However, instead of just searching for a shape analogue of one of the conformers of a reference compound, in the case of multiple references, the algorithm performs a search for a compound in the virtual library whose conformers have overlapped with conformers of each of the reference compounds. The latter will increase the chances that the selected virtual compound binds the same way to the corresponding targets of each of the references (*i.e.* the selected compound is capable of forming conformations that resemble active conformations responsible for the MoA of each of the references).

Performance-wise, in comparison with explicit 3D alignment methods, MultiRef3D exhibits speed-ups closely resembling those achieved by USR-CAT (which is at the core of the MultiRef3D methodology) and scales linearly with the number of reference compounds in the query. Also, since the number of top hits for each reference (typically in the range 1,000–10,000) is set to be orders of magnitude lower than the number of compounds in the screening universe, the final step (hits scores summation and sorting) takes less than a millisecond on any modern single CPU (*e.g.* Intel Core i7). The comparative performance in relative units are summarized and presented in [Table 1](#).

Method case study validation for known targets

To case study validate the proposed methodology for the multi-target-specific conformer similarity the three following targets have been used: 3CLpro (Mpro), PLpro, and RdRp of the SARS-CoV-2. The spike protein has not been included as the validation target since the pharmacological activity may not be correlated directly with the binding affinity to the interfacial site ([Murugan et al., 2020](#)). ChEMBL (version 28) public database ([Gaulton et al., 2011](#)) has been chosen as the universe for screening. The selected ChEMBL

Table 1 The comparative performance of hit identification via different methods with MultiRef3D search time presented in relative time units. The search setup is identical to that described in *Ballester & Richards (2007a)*.

Method	Performance (Relative Time Units)
MultiRef3D	1
EShape3D	515
Shape signatures	679
ROCS	4745

compounds were already marketed drugs for which at least one target is known. The corresponding ChEMBL extraction query is provided in the code available on GitHub (<https://github.com/quantori/MultiRef3D>). The screened set had a total of 2,604 compounds. The corresponding reference compounds for case study validation were selected from the recent multi-target *in silico* repurposing study (*Murugan et al., 2020*) based on the highest binding affinities for each of the targets.

Compounds search based on the conformers of the reference compounds

One hundred conformers for each of the reference molecules were generated at the MMFF94 (*Halgren, 1996*) and each conformer was ODDT-fingerprinted (*Wójcikowski et al., 2019*) and saved in the MongoDB database (*MongoDB, 2020*). The ODDT implementation (*Wójcikowski et al., 2019*) of ElectroShape fingerprints (*Armstrong et al., 2010*) has been selected to demonstrate the proposed approach because these fingerprints are considered to be state-of-the-art in ligand-based virtual screening experiments (*Cortés-Cabrera et al., 2013; Bonanno & Ebejer, 2020*), and they are not limited to binary values.

Virtual libraries for screening

Virtual libraries (query compounds) for screening consisted of an Enamine (*Enamine, 2020*) focused “antiviral-like” set (3995 compounds) and a diverse Discovery Diversity Set (10559 compounds) (*Enamine, 2020*). Molecules from each virtual library were simultaneously evaluated against several reference drugs with different MoA (3CLpro, PLpro and RdRp inhibition). A query molecule for which some of its conformers are similar in shape to conformers for all the reference drugs would receive a higher score. In this approach, multiple virtual compounds can be identified to have a good conformer overlap with the conformers of reference drugs.

RESULTS

Method case study validation for SARS-CoV-2 Compounds

The highest affinity binder Olaparib (−9.2 kcal/mol) has been selected as a reference compound for 3CLpro, Tadalafil (−9.2 kcal/mol) for PLpro and Lumacaftor (−9.9 kcal/mol) for RdRp. However, when multi-target scoring against these three references has been performed, the top ten scoring compounds from ChEMBL *had no conformers* similar in 3D shape (Euclidean distance < 0.5) to Lumacaftor conformers. Therefore, the

Table 2 Top ten scoring compounds showing simultaneous conformer similarity with the reference compounds Olaparib, Tadalafil, and Ergotamine.

Compound ID	Compound Name	TotalScore	Olaparib	Tadalafil	Ergotamine
CHEMBL779	Tadalafil	228.46	70.70	100.00	57.76
CHEMBL1737	Sildenafil citrate	225.15	81.30	58.34	85.50
CHEMBL521686	Olaparib	223.08	100.00	57.61	65.48
CHEMBL105442	Ci-1040	220.40	80.68	79.16	60.56
CHEMBL129857	As-602868	220.16	78.27	74.50	67.39
CHEMBL2037511	Epelsiban	219.86	81.58	70.28	68.01
CHEMBL565612	Sotrastaurin	219.13	79.93	69.36	69.83
CHEMBL1516474	Tegaserod maleate	217.83	80.22	76.56	61.05
CHEMBL1236682	Refametinib	217.78	76.01	81.57	60.20
CHEMBL1923502	Ulimorelin hydrochloride	217.56	76.29	74.79	66.47

Lumacaftor reference has been replaced with the next best *in silico* RdRp binder Ergotamine (Murugan *et al.*, 2020) (−9.4 kcal/mol). The resulting scores produced by the proposed method are summarized in Table 2.

Both Olaparib and Tadalafil had the highest scores which confirmed the previous finding (Murugan *et al.*, 2020) that these compounds are simultaneously good binders for both 3CLpro and PLpro. Our method has also picked up Sildenafil (brand name Viagra) which just like Tadalafil (Cialis) is also known as a classical PDE5A inhibitor. Although those compounds are predominantly used in the treatment of male erectile dysfunction and pulmonary hypertension, it was shown (Shirvaliloo, 2021) that in the presence of SARS-CoV-2 infection, PDE5 inhibitors prevent thromboembolism caused by inflammatory processes in COVID-19 patients via NO/cGMP pathway and are potent inhibitors of 3CLpro (Jin *et al.*, 2020)

Ci-1040 and Refametinib are the other two hits from Table 2 and are potent MEK inhibitors with high 3D shape similarity to both Olaparib and Tadalafil. MEK inhibitors, including Olaparib (Vena *et al.*, 2018) were recently demonstrated to reduce cellular expression of ACE2 while stimulating NK-mediated cytotoxicity and attenuating inflammatory cytokines during the severe stage of SARS-CoV-2 infection (Zhou *et al.*, 2020). Ci-1040 was also previously shown to display a broad anti-influenza virus activity *in vitro* and to provide a prolonged treatment window compared to the standard of care *in vivo*, specifically in lung cells (Haasbach *et al.*, 2017).

The other hit from Table 2 is Sotrastaurin, a PKC inhibitor that has been experimentally shown to inhibit SARS-CoV-2 replication *in vivo* (Liu *et al.*, 2021) and found to be among the best 3CLpro binders during *in silico* ZINC database screening study (Olubiyi *et al.*, 2020). The other top hit, Epelsiban, was originally developed as an oxytocin receptor agonist. However, it has been recently shown (Kim *et al.*, 2015) that oxytocin plays a major role in the activation of NF-κB-mediated pathways. Interestingly, recent research has revealed (Hariharan *et al.*, 2021) that Remdesivir, in addition to being a potent RdRp inhibitor (Gordon *et al.*, 2020), is also reducing viral replication via NF-κB pathway. Therefore, this hit serves as an example of non-obvious 3D-shape-based drug repurposing

Table 3 Top ten scoring compounds showing simultaneous conformer similarity with the reference compounds Olaparib, Tadalafil, and Remdesivir.

Compound ID	Compound Name	TotalScore	Olaparib	Tadalafil	Remdesivir
CHEMBL1694	Benazepril hydrochloride	180.82	66.67	64.26	49.89
CHEMBL515606	Cilazapril	180.61	64.56	61.56	54.50
CHEMBL495727	At-9283	179.03	68.17	56.15	54.71
CHEMBL2107495	Temafloxacin hydrochloride	178.94	67.15	55.78	56.01
CHEMBL1200779	Trovaflaxacin mesylate	178.60	66.24	54.02	58.35
CHEMBL340978	Benoxaprofen	178.27	68.56	56.54	53.16
CHEMBL8	Ciprofloxacin	177.05	63.21	57.19	56.65
CHEMBL1200831	Spirapril hydrochloride	177.00	65.28	60.24	51.47
CHEMBL1201011	Quinapril hydrochloride	176.84	66.32	60.40	50.13
CHEMBL1168	Ramipril	176.54	65.32	63.26	47.96

idea generation linked to the relevant yet non-primary SARS-CoV-2 inhibiting mechanisms of reference compounds.

In our second case study validation experiment, we explored what happens if the RdRp reference compound Ergotamine is replaced with Remdesivir which, as was already mentioned, is not only a well-established RdRp inhibitor and computationally found to be a tight RdRp binder but also a cytokine storm attenuator that works via NF-kB pathway. We were interested if the algorithm would pick up NF-kB hits and other potential “chain terminators”. The resulting scores produced in the second scoring setup are summarized in [Table 3](#).

For Olaparib, Tadalafil, and Remdesivir reference compounds, half of the top ten hits (Benoxaprofen, Ciprofloxacin, Spirapril hydrochloride, Quinapril hydrochloride and Ramipril) turned out to be ACE inhibitors and coagulation modifiers acting via NF-kB related pathways ([Hernández-Presa et al., 1997](#); [Burzynski et al., 2019](#))! In addition, all of them turned out to be also good binders of 3CLpro ([Biembengut & Brasil de Souza, 2020](#)). One can also notice that the individual scores for Remdesivir-only hits are *significantly* (>10%) lower than the corresponding scores for the other reference compounds, which can be readily explained by the fact that none of the ChEMBL hits was a nucleoside and thus cannot be incorporated into the replicated RNA similar to the way Remdesivir does (although we still pick up the NF-kB component from Remdesivir’s MoA).

The other hits were Temafloxacin and Trovaflaxacin, predicted to be potent 3CLpro ligands ([Gimeno et al., 2020](#)) and experimentally shown to inhibit virus replication ([Krieg et al., 2006](#); [Mirmotalebioshi et al., 2021](#)) and anti-inflammatory drugs Benoxaprofen and Ciproflaxin predicted to target 3CLpro ([Marciniec et al., 2020](#); [Zeyrek et al., 2021](#)) as well.

An interesting multi-target Aurora/JAK inhibitor, compound At-9283, closes the list ([Table 3](#)). JAK inhibitors have promising therapeutic potential for SARS-CoV-2 treatment with their dual anti-inflammatory and anti-viral effects ([Mehta et al., 2020](#)). At-9283 has also been recently identified to reverse SARS-CoV-2 transcriptomic signature ([O’Donovan et al., 2020](#)) and due to its similarity to tipiracil 3D pharmacophore scaffold, also inhibits

SARS-CoV-2 Nsp15 endoribonuclease (*Kandwal & Fayne, 2020; Guedes et al., 2021*) and targets 3CLpro (*Mengist, Dilnessa & Jin, 2021; Baby et al., 2021*).

In summary, the results of these case study validation experiments show that MultiRef3D can efficiently identify compounds whose conformers simultaneously mimic the conformers of three different small molecules. All identified high-score compounds represent drugs that have direct or indirect evidence to be effective in anti-COVID-19 treatment.

Virtual library screening for multi-target SARS-CoV-2 compounds

The results from the focused (“antiviral-like”) and diverse (“Discovery Diversity Set”) sets are summarized in [Tables 1](#) and [2](#) respectively. These are given here for illustrative purposes only, to demonstrate that the hits are indeed simultaneously aligned with the references. The algorithm visual summary is displayed in [Fig. 1](#) for the W_{All} objective function. [Tables S1](#) and [S2](#) summarize the direct application results of the Enamine (*Enamine, 2020*) focused “antiviral-like” and “Diverse Discovery Set” virtual library screening. The first two columns of the Tables contain query compound IDs and their computed overlap scores. The rows are sorted according to the total sum overlap score displayed in the second column.

For the visual illustration of the algorithm results, the two compounds with the highest scores from [Tables S1](#) and [S2](#) have been presented in [Fig. 2](#). It is worth noting that these compounds are quite flexible molecules due to their amide bridge around which the ring substructures can rotate, which ensures the ability of those molecules to accommodate different targets. One can also notice that the Remdesivir component scores are significantly lower in comparison to other references (while Ergotamine component remains high), reflective of the facts that, just as in ChEMBL case, none of the hits was a nucleoside in nature (see also [Fig. 3D](#)).

The best-matching conformers of the top hit Z1693453146 spatially align with the active conformation for each reference drug ([Fig. 3](#)). One can observe that most of hydrogen donors and acceptors from the top hit conformer and reference conformers are aligned very well, mimicking the interaction patterns with each target. At least partial spatial alignment of atom types is expected from the top hit conformers since atom types as well as their relative 3D positions is the essence of the USRCAT fingerprints (*Schreyer & Blundell, 2012*).

DISCUSSION

Computation efficiency and availability of the method

The proposed method does not rely on laborious docking and molecular dynamics setup, especially in the multi-target case, where target preparation and choice of method *i.e.* direct docking to a fixed-coordinate target or Molecular Dynamics-based ensemble energy minimization are of utmost importance and require deep expertise. Fingerprint comparison is orders of magnitude faster and simpler; it only requires simple structural information in the form of either isomeric SMILES or InChI. The entire setup, which is presented in the [Supplementary Information](#), can be universally used for any multi-target screening and optimization, whenever reference compounds for each of the targets are available.

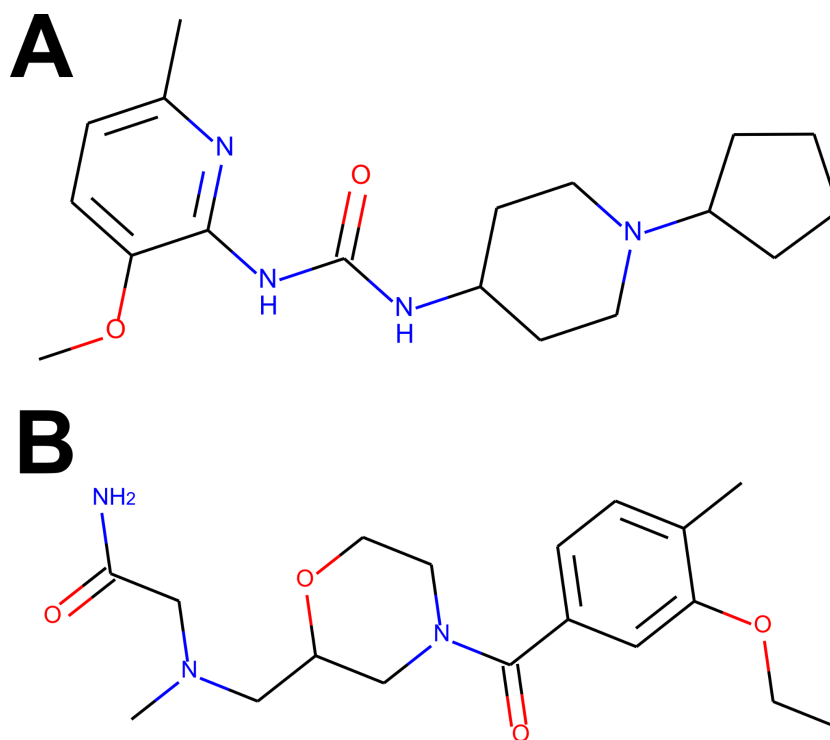


Figure 2 The compounds presented in panels A and B are the top hits Z1693453146 ($Wall = 254.11$) and ZZ1760146546 ($Wall = 255.19$) from the non-overlapping “antiviral-like” and “Discovery Diversity” libraries, respectively. One can immediately observe, however, that the compounds share a lot of similarity, in particular overall shape and amide bridge connecting heterocycles. The bridge allows for 3D flexibility for the molecule to change conformation and bind to multiple targets. The figure has been created in Microsoft PowerPoint 2016, pyMOL v2.5 (pymol.org) and RDKit v2021.03.01 software (rdkit.org). Full-size DOI: [10.7717/peerj.14252/fig-2](https://doi.org/10.7717/peerj.14252/fig-2)

Naturally, further hit refinement (ADMETox, PK/PD, *etc*) is necessary if the screened universe is not limited to drugs with well-known safety profiles.

Depending on what is known about the indication or marketed drug of interest (targets, MoAs, other existing drugs for the same indication), the proposed methods (or a combination thereof) can be used to find other non-obvious molecules whose shape and surface electrostatic charge is similar to that of the marketed drug. The methods can also be used to search for the cumulative similarity to conformers of the multiple drugs used to treat this disease indication.

In the proposed approach multiple conformers of the query ligand have been compared with conformers from *multiple* reference compounds whose therapeutic effect of interest is achieved via different mechanisms of bindings to different targets, *e.g.* by inhibiting major proteases 3CLpro and PLpro (Ullrich & Nitsche, 2020) and RNA-dependent RNA polymerase (RdRp) (Elfiky, 2020; Li *et al.*, 2003; Vincent *et al.*, 2005). An “ideal drug” would contain conformers that resemble (as many as possible) conformers of all the reference drugs, thus increasing chances that the drug inhibits SARS-CoV-2 via multi-MoA routes and is more effective than each individual reference drug.

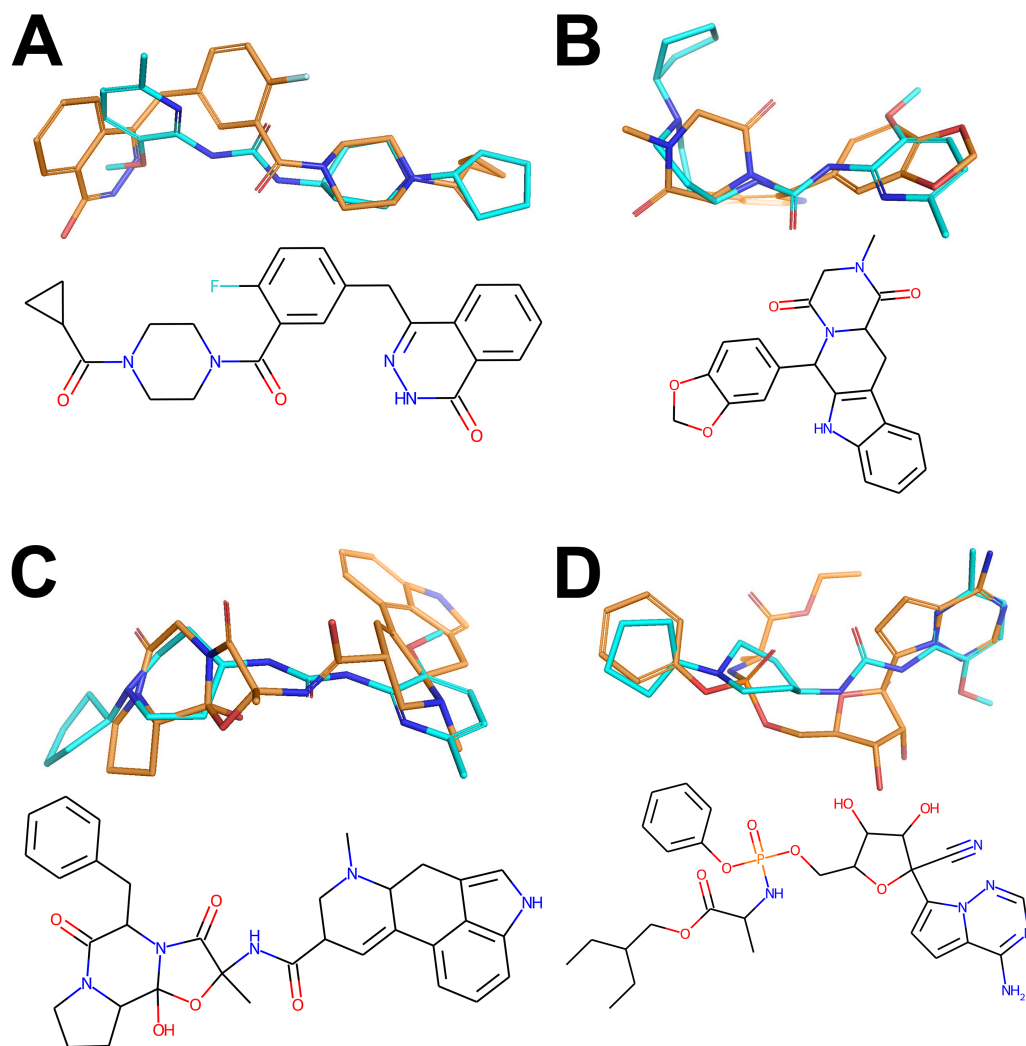


Figure 3 Active conformers of the Reference compounds (Olaparib, Tadalafil, Ergotamine and Remdesivir on A, B, C and D, respectively) aligned with the best matching conformers of the top hit Z1693453146 (Wall = 254.11). Carbon-carbon bonds for the reference compounds and the Top Hit are shown in gold and cyan respectively (C-N and C-O bonds are conventionally shown in blue and red). The figure has been created in Microsoft PowerPoint 2016, pyMOL v2.5 (pymol.org), RDKit v2021.03.01 software (rdkit.org) and Adobe Photoshop CC v20.0.6.

Full-size DOI: 10.7717/peerj.14252/fig-3

When the crystal structure of the target protein is known and the reference ligand is co-crystallized in its active conformation (structure-based design), we can use this information about the reference compound and evaluate the query molecules against only one, the active (co-crystallized), reference ligand conformation ($r = r_{active}$) in formulas Eqs. (1) and (2). Confirmation by direct docking for the fingerprint-matched queries can be used to confirm the match.

Our methodology emphasizes the pursuit of candidate compounds that achieve the therapeutic effect (e.g. stops SARS-CoV-2 proliferation) by multiple MoA routes. A

successful candidate compound would contain conformers targeting the three SARS-CoV-2 factors (3CLpro, PLpro, RdRpall) at the same time by increasing the chances that the compound would protect against SARS-CoV-2 much more effectively. Naturally, all successful candidates would need to be further screened and filtered for proper ADME-Tox and other drug-likeness properties. Binding to anti-targets, *e.g.* hERG, can be explicitly incorporated into this methodology by adding the corresponding terms (similarities to known hERG-binding ligands) to the overlap sum with a negative sign. Even though many computational methods exist to evaluate hERG in particular as well as other common tox liabilities, when an anti-target is very specific and less commonly known as “pure tox target” (*e.g.* undesired binding to D2 receptor for many modern CNS drugs), the explicit inclusion of similarity score to such anti-target with a negative sign can greatly streamline the overall drug optimization process.

CONCLUSIONS

We have demonstrated and case study validated the usefulness of the multi-reference computationally efficient optimization approach in drug discovery screening and repurposing scenarios. The method represents each molecule as an ensemble of flexible conformers that would choose the best possible conformation for each presented target-binding opportunity. The application of this approach to SARS-CoV-2 produced several antiviral drug candidates that are designed to protect against SARS-CoV-2 by multiple mechanisms simultaneously.

List of Abbreviations

ADME-Tox	Absorption, Distribution, Metabolism, Excretion and Toxicity
GPU	Graphics processing unit
CNS	Central nervous system
CoMFA	Comparative molecular field analysis
COVID-19	Coronavirus Disease of 2019
CPU	Central processing unit
hERG	Human Ether-a-go-go-related Gene
MoA(s)	Mechanism of Action(s)
ODDT	Open Drug Discovery Toolkit
RNA	Ribonucleic acid
ROCS	Rapid overlay of chemical structures
SARS-CoV-2	Severe acute respiratory syndrome coronavirus 2
USR	Ultrafast Shape Recognition
WHO	World Health Organization

ACKNOWLEDGEMENTS

The authors would like to acknowledge Nika Tsutskiridze and Daviti Khatchilava for their assistance in extracting information from clinical trials and peer reviewed literature. The authors also want to acknowledge Alex Proutski and John Reynders for their suggestions, comments and help during the manuscript preparation, writing and revisions.

ADDITIONAL INFORMATION AND DECLARATIONS

Funding

Quantori LLC provided support in the form of salaries for Omar Kantidze and Yuriy Gankin as well as relevant publication and patent fees. The funders had no role in study design, data collection and analysis, decision to publish, or preparation of the manuscript.

Grant Disclosures

The following grant information was disclosed by the authors:
Quantori LLC, publication and patent fees.

Competing Interests

Vadim Alexandrov is a founder of a consulting for-profit company Liquid Algo LLC located in Hopewell Junction, New York, United States and received salary for his work while working as a consultant for Quantori LLC. Alexander Kirpich is employed by the School of Public Health in non-profit Georgia State University in Atlanta, Georgia, United States. Omar Kantidze and Yuriy Gankin are employed by a commercial for-profit company Quantori LLC, Cambridge, Massachusetts, United States. The proposed method has been submitted for a patent. The patent application number is 63061790 at the United States Patent and Trademark Office and as of October 17, 2020, the patent is pending.

The patent can be a source of financial income for authors Vadim Alexandrov (VA) and Yuriy Gankin (YG).

Author Contributions

- Vadim Alexandrov conceived and designed the experiments, performed the experiments, analyzed the data, prepared figures and/or tables, authored or reviewed drafts of the article, and approved the final draft.
- Alexander Kirpich conceived and designed the experiments, prepared figures and/or tables, authored or reviewed drafts of the article, and approved the final draft.
- Omar Kantidze conceived and designed the experiments, prepared figures and/or tables, authored or reviewed drafts of the article, and approved the final draft.
- Yuriy Gankin conceived and designed the experiments, authored or reviewed drafts of the article, and approved the final draft.

Patent Disclosures

The following patent dependencies were disclosed by the authors:

The proposed method (MultiRef3D) has been submitted for a patent. The World Intellectual Property Organization (WIPO) Patent Application Number is WO/2022/032044. The International Application No. is PCT/US2021/044857. The patent information is available at <https://patentscope.wipo.int/search/en/search.jsf>.

Data Availability

The following information was supplied regarding data availability:

The code used for analysis is available at the Quantori GitHub repository: <https://github.com/quantori/MultiRef3D> and via Zenodo DOI: <https://doi.org/10.5281/zenodo.7261953>.

The data (ligand structures) from REAL focused libraries is available at the Enamine Ltd: <https://enamine.net/compound-collections/real-compounds/real-database>; <https://doi.org/10.1002/ejoc.202101210>.

Supplemental Information

Supplemental information for this article can be found online at <http://dx.doi.org/10.7717/peerj.14252#supplemental-information>.

REFERENCES

- Acharya C, Coop A, Polli JE, Mackerell Jr AD. 2011.** Recent advances in ligand-based drug design: relevance and utility of the conformationally sampled pharmacophore approach. *Current Computer-Aided Drug Design* 7:10–22 DOI 10.2174/157340911793743547.
- Armstrong MS, Morris GM, Finn PW, Sharma R, Moretti L, Cooper RI, Richards WG. 2010.** ElectroShape: fast molecular similarity calculations incorporating shape, chirality and electrostatics. *Journal of Computer-Aided Molecular Design* 24:789–801 DOI 10.1007/s10822-010-9374-0.
- Axen SD, Huang X-P, Cáceres EL, Gendeleev L, Roth BL, Keiser MJ. 2017.** A simple representation of three-dimensional molecular structure. *Journal of Medicinal Chemistry* 60:7393–7409 DOI 10.1021/acs.jmedchem.7b00696.
- Baby K, Maity S, Mehta CH, Suresh A, Nayak UY, Nayak Y. 2021.** Targeting SARS-CoV-2 main protease: a computational drug repurposing study. *Archives of Medical Research* 52:38 DOI 10.1016/j.arcmed.2020.09.013.
- Bajusz D, Rácz A, Héberger K. 2015.** Why is Tanimoto index an appropriate choice for fingerprint-based similarity calculations? *Journal of Cheminformatics* 7:1 DOI 10.1186/s13321-014-0049-z.
- Ballester PJ, Richards WG. 2007a.** Ultrafast shape recognition for similarity search in molecular databases. *Proceedings of the Royal Society A: Mathematical, Physical and Engineering Sciences* 463:1307–1321 DOI 10.1098/rspa.2007.1823.
- Ballester PJ, Richards WG. 2007b.** Ultrafast shape recognition to search compound databases for similar molecular shapes. *Journal of Computational Chemistry* 28:1711–1723 DOI 10.1002/jcc.20681.
- Biembengut IV, Brasil de Souza TdA. 2020.** Coagulation modifiers targeting SARS-CoV-2 main protease Mpro for COVID-19 treatment: an in silico approach. *Memorias do Instituto Oswaldo Cruz* 115:e200179 DOI 10.1590/0074-02760200179.
- Blaney JM, Scott Dixon J. 2007.** Distance geometry in molecular modeling. *Reviews in Computational Chemistry* 5:299–335 DOI 10.1002/9780470125823.ch6.
- Bonanno E, Ebejer J-P. 2020.** Applying machine learning to ultrafast shape recognition in ligand-based virtual screening. *Frontiers in Pharmacology* 10:1–8 DOI 10.3389/fphar.2019.01675.
- Burzynski LC, Humphry M, Pyryllou K, Wiggins KA, Chan JNE, Figg N, Kitt LL, Summers C, Tatham KC, Martin PB, Bennett MR, Clarke MCH. 2019.** The coagulation

- and immune systems are directly linked through the activation of interleukin-1 α by thrombin. *Immunity* **50**:1033–1042.e6 DOI 10.1016/j.immuni.2019.03.003.
- Cappel D, Dixon SL, Sherman W, Duan J. 2014.** Exploring conformational search protocols for ligand-based virtual screening and 3-D QSAR modeling. *Journal of Computer-Aided Molecular Design* **29**:165–182.
- Chen Y, Yuan X, Xiao Z, Jin H, Zhang L, Liu Z. 2018.** Discovery of novel multidrug resistance protein 4 (MRP4) inhibitors as active agents reducing resistance to anticancer drug 6-Mercaptopurine (6-MP) by structure and ligand-based virtual screening. *PLOS ONE* **13**(10):e0205175 DOI 10.1371/journal.pone.0205175.
- Cortés-Cabrera A, Morris GM, Finn PW, Morreale A, Gago F. 2013.** Comparison of ultra-fast 2D and 3D ligand and target descriptors for side effect prediction and network analysis in polypharmacology. *British Journal of Pharmacology* **170**:557–567 DOI 10.1111/bph.12294.
- Elfiky AA. 2020.** SARS-CoV-2 RNA dependent RNA polymerase (RdRp) targeting: an perspective. *Journal of Biomolecular Structure & Dynamics* **39**(9):3204–3212 DOI 10.1080/07391102.2020.1761882.
- Enamine. 2020.** REAL Database-Enamine. Available at <https://enamine.net/library-synthesis/real-compounds/real-database> (accessed on 15 October 2020).
- Friedrich N-O, de Bruyn Kops C, Flachsenberg F, Sommer K, Rarey M, Kirchmair J. 2017a.** Benchmarking commercial conformer ensemble generators. *Journal of Chemical Information and Modeling* **57**:2719–2728 DOI 10.1021/acs.jcim.7b00505.
- Friedrich N-O, Meyder A, de Bruyn Kops C, Sommer K, Flachsenberg F, Rarey M, Kirchmair J. 2017b.** High-quality dataset of protein-bound ligand conformations and its application to benchmarking conformer ensemble generators. *Journal of Chemical Information and Modeling* **57**:529–539 DOI 10.1021/acs.jcim.6b00613.
- Gaulton A, Bellis LJ, Bento AP, Chambers J, Davies M, Hersey A, Light Y, McGlinchey S, Michalovich D, Al-Lazikani B, Overington JP. 2011.** ChEMBL: a large-scale bioactivity database for drug discovery. *Nucleic Acids Research* **40**(Database issue):D1100-7 DOI 10.1093/nar/gkr777.
- Geman S, Geman D. 1984.** Stochastic relaxation, gibbs distributions, and the bayesian restoration of images. *IEEE Transactions on Pattern Analysis and Machine Intelligence* **6**:721–741 DOI 10.1109/tpami.1984.4767596.
- Gimeno A, Mestres-Truyol J, Ojeda-Montes MJ, Macip G, Saldivar-Espinoza B, Cereto-Massagué A, Pujadas G, Garcia-Vallvé S. 2020.** Prediction of novel inhibitors of the main protease (M-pro) of SARS-CoV-2 through consensus docking and drug reposition. *International Journal of Molecular Sciences* **21**:3793 DOI 10.3390/ijms21113793.
- Gladysz R, Dos Santos FM, Langenaeker W, Thijs G, Augustyns K, De Winter H. 2018.** Spectrophores as one-dimensional descriptors calculated from three-dimensional atomic properties: applications ranging from scaffold hopping to multi-target virtual screening. *Journal of Cheminformatics* **10**:9 DOI 10.1186/s13321-018-0268-9.
- Gohda K, Mori I, Ohta D, Kikuchi T. 2000.** *Journal of Computer-Aided Molecular Design* **14**:265–275 DOI 10.1023/A:1008193217627.

- Gordon CJ, Tchesnokov EP, Woolner E, Perry JK, Feng JY, Porter DP, Götte M. 2020.** Remdesivir is a direct-acting antiviral that inhibits RNA-dependent RNA polymerase from severe acute respiratory syndrome coronavirus 2 with high potency. *The Journal of Biological Chemistry* **295**:6785–6797 DOI [10.1074/jbc.RA120.013679](https://doi.org/10.1074/jbc.RA120.013679).
- Grant JA, Gallardo MA, Pickup BT. 1996.** A fast method of molecular shape comparison: a simple application of a Gaussian description of molecular shape. *Journal of Computational Chemistry* **17**:1653–1666 DOI [10.1002/\(SICI\)1096-987X\(19961115\)17:14<1653::AID-JCC7>3.0.CO;2-K](https://doi.org/10.1002/(SICI)1096-987X(19961115)17:14<1653::AID-JCC7>3.0.CO;2-K).
- Guedes IA, Costa LSC, Dos Santos KB, Karl ALM, Rocha GK, Teixeira IM, Galheigo MM, Medeiros V, Krempser E, Custódio FL, Barbosa HJC, Nicolás MF, Dardenne LE. 2021.** Drug design and repurposing with DockThor-VS web server focusing on SARS-CoV-2 therapeutic targets and their non-synonym variants. *Scientific Reports* **11**:5543 DOI [10.1038/s41598-021-84700-0](https://doi.org/10.1038/s41598-021-84700-0).
- Haasbach E, Müller C, Ehrhardt C, Schreiber A, Pleschka S, Ludwig S, Planz O. 2017.** The MEK-inhibitor CI-1040 displays a broad anti-influenza virus activity *in vitro* and provides a prolonged treatment window compared to standard of care *in vivo*. *Antiviral Research* **142**:178–184 DOI [10.1016/j.antiviral.2017.03.024](https://doi.org/10.1016/j.antiviral.2017.03.024).
- Halgren TA. 1996.** Merck molecular force field, I. Basis, form, scope, parameterization, and performance of MMFF94. *Journal of Computational Chemistry* **17**:490–519 DOI [10.1002/\(SICI\)1096-987X\(199604\)17:5/6<490::AID-JCC1>3.0.CO;2-P](https://doi.org/10.1002/(SICI)1096-987X(199604)17:5/6<490::AID-JCC1>3.0.CO;2-P).
- Haque IS, Pande VS. 2010.** PAPER—accelerating parallel evaluations of ROCS. *Journal of Computational Chemistry* **31**:117–132 DOI [10.1002/jcc.21307](https://doi.org/10.1002/jcc.21307).
- Hariharan A, Hakeem AR, Radhakrishnan S, Reddy MS, Rela M. 2021.** The role and therapeutic potential of NF-kappa-B pathway in severe COVID-19 patients. *Inflammopharmacology* **29**(1):91–100 DOI [10.1007/s10787-020-00773-9](https://doi.org/10.1007/s10787-020-00773-9).
- Hasegawa K, Arakawa M, Funatsu K. 2000.** Rational choice of bioactive conformations through use of conformation analysis and 3-way partial least squares modeling. *Chemometrics and Intelligent Laboratory Systems* **50**:253–261 DOI [10.1016/S0169-7439\(99\)00063-5](https://doi.org/10.1016/S0169-7439(99)00063-5).
- Hawkins PCD, Skillman AG, Nicholls A. 2007.** Comparison of shape-matching and docking as virtual screening tools. *Journal of Medicinal Chemistry* **50**:74–82 DOI [10.1021/jm0603365](https://doi.org/10.1021/jm0603365).
- Hernández-Presa M, Bustos C, Ortego M, Tuñón J, Renedo G, Ruiz-Ortega M, Egido J. 1997.** Angiotensin-converting enzyme inhibition prevents arterial nuclear factor-kappa B activation, monocyte chemoattractant protein-1 expression, and macrophage infiltration in a rabbit model of early accelerated atherosclerosis. *Circulation* **95**:1532–1541 DOI [10.1161/01.cir.95.6.1532](https://doi.org/10.1161/01.cir.95.6.1532).
- Jin Z, Du X, Xu Y, Deng Y, Liu M, Zhao Y, Zhang B, Li X, Zhang L, Peng C, Duan Y, Yu J, Wang L, Yang K, Liu F, Jiang R, Yang X, You T, Liu X, Yang X, Bai F, Liu H, Liu X, Guddat LW, Xu W, Xiao G, Qin C, Shi Z, Jiang H, Rao Z, Yang H. 2020.** Structure of M pro from SARS-CoV-2 and discovery of its inhibitors. *Nature* **582**:289–293 DOI [10.1038/s41586-020-2223-y](https://doi.org/10.1038/s41586-020-2223-y).

- Kandwal S, Fayne D. 2020.** Repurposing drugs for treatment of SARS-CoV-2 infection: computational design insights into mechanisms of action. *Journal of Biomolecular Structure and Dynamics* **40**(3):1316–1330 DOI [10.1080/07391102.2020.1825232](https://doi.org/10.1080/07391102.2020.1825232).
- Khan SU, Ahemad N, Chuah L-H, Naidu R, Thet Htar T. 2019.** Sequential ligand- and structure-based virtual screening approach for the identification of potential G protein-coupled estrogen receptor-1 (GPER-1) modulators. *RSC Advances* **9**(5):2525–2538 DOI [10.1039/C8RA09318K](https://doi.org/10.1039/C8RA09318K).
- Kim SH, MacIntyre DA, Da Silva MF, Blanks AM, Lee YS, Thornton S, Bennett PR, Terzidou V. 2015.** Oxytocin activates NF- κ B-mediated inflammatory pathways in human gestational tissues. *Molecular and Cellular Endocrinology* **403**(5):64–77 DOI [10.1016/j.mce.2014.11.008](https://doi.org/10.1016/j.mce.2014.11.008).
- Kirchmair J, Distinto S, Markt P, Schuster D, Spitzer GM, Liedl KR, Wolber G. 2009.** How to optimize shape-based virtual screening: choosing the right query and including chemical information. *Journal of Chemical Information and Modeling* **49**:678–692 DOI [10.1021/ci8004226](https://doi.org/10.1021/ci8004226).
- Krieg A, Schetter C, Bratzler R, Vollmer J, Jurk M, Bauer S. 2006.** Methods and products for enhancing immune responses using imidazoquinoline compounds (US20060188913A1). US patent. Available at <https://patents.google.com/patent/US20060188913A1/en>.
- Kumar A, Ito A, Takemoto M, Yoshida M, Zhang KYJ. 2014.** Identification of 1, 2, 5-oxadiazoles as a new class of SENP2 inhibitors using structure based virtual screening. *Journal of Chemical Information and Modeling* **54**(3):870–880 DOI [10.1021/ci4007134](https://doi.org/10.1021/ci4007134).
- Kumar A, Ito A, Takemoto M, Yoshida M, Zhang KYJ. 2014.** Identification of new SUMO activating enzyme 1 inhibitors using virtual screening and scaffold hopping. *Bioorganic & Medicinal Chemistry Letters* **26**(4):1218–1223 DOI [10.1016/j.bmcl.2016.01.030](https://doi.org/10.1016/j.bmcl.2016.01.030).
- Li W, Moore MJ, Vasilieva N, Sui J, Wong SK, Berne MA, Somasundaran M, Sullivan JL, Luzuriaga K, Greenough TC, Choe H, Farzan M. 2003.** Angiotensin-converting enzyme 2 is a functional receptor for the SARS coronavirus. *Nature* **426**:450–454 DOI [10.1038/nature02145](https://doi.org/10.1038/nature02145).
- Liu S, Zhu L, Xie G, Mok BW-Y, Yang Z, Deng S, Lau S-Y, Chen P, Wang P, Chen H, Cai Z. 2021.** Potential antiviral target for SARS-CoV-2: a key early responsive kinase during viral entry. *CCS Chemistry* **4**:559–568 DOI [10.31635/ccschem.021.202000603](https://doi.org/10.31635/ccschem.021.202000603).
- Mackerell Jr AD. 2004.** Empirical force fields for biological macromolecules: overview and issues. *Journal of Computational Chemistry* **25**:1584–1604 DOI [10.1002/jcc.20082](https://doi.org/10.1002/jcc.20082).
- Marciniak K, Beberok A, Pęcak P, Boryczka S, Wrześniak D. 2020.** Ciprofloxacin and moxifloxacin could interact with SARS-CoV-2 protease: preliminary in silico analysis. *Pharmacological Reports* **72**(6):1553–1561 Epub 2020 Oct 15 DOI [10.1007/s43440-020-00169-0](https://doi.org/10.1007/s43440-020-00169-0).

- Mehta P, Ciurtin C, Scully M, Levi M, Chambers RC. 2020.** JAK inhibitors in COVID-19: the need for vigilance regarding increased inherent thrombotic risk. *The European Respiratory Journal* **56**:2001919 DOI [10.1183/13993003.01919-2020](https://doi.org/10.1183/13993003.01919-2020).
- Mengist HM, Dilnessa T, Jin T. 2021.** Structural basis of potential inhibitors targeting SARS-CoV-2 main protease. *Frontiers in Chemistry* **9**:622898 DOI [10.3389/fchem.2021.622898](https://doi.org/10.3389/fchem.2021.622898).
- Mirmotalebioshi SA, Adibi A, Sameni M, Karami F, Niazi V, Niknam Z, Aliashrafi M, Taheri M, Ghafouri-Fard J, Jeibouei S, Mahdian S, Zali H, Ranjbar MM, Yazdani M. 2021.** Identification of FDA approved drugs against SARS-CoV-2 RNA dependent RNA polymerase (RdRp) and 3-chymotrypsin-like protease (3CLpro), drug repurposing approach. *Biomedicine & Pharmacotherapy* **138**:111544 DOI [10.1016/j.biopha.2021.111544](https://doi.org/10.1016/j.biopha.2021.111544).
- MongoDB. 2020.** MongoDB Atlas Database. Available at <https://www.mongodb.com> (accessed on 15 October 2020).
- Murugan NA, Kumar S, Jeyakanthan J, Srivastava V. 2020.** Searching for target-specific and multi-targeting organics for Covid-19 in the Drugbank database with a double scoring approach. *Scientific Reports* **10**(1):19125 DOI [10.1038/s41598-019-56847-4](https://doi.org/10.1038/s41598-019-56847-4).
- O'Donovan SM, Eby H, Henkel ND, Creeden J, Imami A, Asah S, Zhang X, Wu X, Alnafisah R, Taylor R, Travis, Reigle J, Thorman A, Shamsaei B, Meller J, McCullumsmith RE. 2020.** Identification of new drug treatments to combat COVID19: a signature-based approach using iLINCS. *Research Square* preprint DOI [10.21203/rs.3.rs-25643/v1](https://doi.org/10.21203/rs.3.rs-25643/v1).
- Olubiyi OO, Olagunju M, Keutmann M, Loschwitz J, Strodel B. 2020.** High throughput virtual screening to discover inhibitors of the main protease of the coronavirus SARS-CoV-2. *Molecules* **25**:3193 DOI [10.3390/molecules25143193](https://doi.org/10.3390/molecules25143193).
- OpenEye Scientific Software, Inc. 2008.** Rapid Overlay of Chemical Structures (ROCS). Santa Fe: OpenEye Scientific Software, Inc.
- OpenEye Scientific Software, Inc. 2011.** FastROCS. Santa Fe: OpenEye Scientific Software, Inc.
- Rush 3rd TS, Grant JA, Mosyak L, Nicholls A. 2005.** A shape-based 3-D scaffold hopping method and its application to a bacterial protein-protein interaction. *Journal of Medicinal Chemistry* **48**:1489–1495 DOI [10.1021/jm040163o](https://doi.org/10.1021/jm040163o).
- Schreyer AM, Blundell T. 2012.** USRCAT: real-time ultrafast shape recognition with pharmacophoric constraints. *Journal of Cheminformatics* **4**:27 DOI [10.1186/1758-2946-4-27](https://doi.org/10.1186/1758-2946-4-27).
- Seep L, Bonin A, Meier K, Diedam H, Göller AH. 2021.** Ensemble completeness in conformer sampling: the case of small macrocycles. *Journal of Cheminformatics* **13**:1–22 DOI [10.1186/s13321-020-00477-w](https://doi.org/10.1186/s13321-020-00477-w).
- Sheridan RP, McGaughey GB, Cornell WD. 2008.** Multiple protein structures and multiple ligands: effects on the apparent goodness of virtual screening results. *Journal of Computer-Aided Molecular Design* **22**:257–265 DOI [10.1007/s10822-008-9168-9](https://doi.org/10.1007/s10822-008-9168-9).

- Shirvaliloo M. 2021.** Targeting the SARS-CoV-2 3CLpro and NO/cGMP/PDE5 pathway in COVID-19: a commentary on PDE5 inhibitors. *Future Cardiology* DOI [10.2217/fca-2020-0201](https://doi.org/10.2217/fca-2020-0201).
- Ullrich S, Nitsche C. 2020.** The SARS-CoV-2 main protease as drug targets. *Bioorganic & Medicinal Chemistry Letters* **30**:127377 DOI [10.1016/j.bmcl.2020.127377](https://doi.org/10.1016/j.bmcl.2020.127377).
- Vena F, Jia R, Esfandiari A, Garcia-Gomez JJ, Rodriguez-Justo M, Ma J, Syed S, Crowley L, Elenbaas B, Goodstal S, Hartley JA, Hochhauser D. 2018.** MEK inhibition leads to BRCA2 downregulation and sensitization to DNA damaging agents in pancreas and ovarian cancer models. *Oncotarget* **9**:11592–11603 DOI [10.18632/oncotarget.24294](https://doi.org/10.18632/oncotarget.24294).
- Venhorst J, Núñez S, Terpstra JW, Kruse CG. 2008.** Assessment of scaffold hopping efficiency by use of molecular interaction fingerprints. *Journal of Medicinal Chemistry* **51**:3222–3229 DOI [10.1021/jm8001058](https://doi.org/10.1021/jm8001058).
- Vincent MJ, Bergeron E, Benjannet S, Erickson BR, Rollin PE, Ksiazek TG, Seidah NG, Nichol ST. 2005.** Chloroquine is a potent inhibitor of SARS coronavirus infection and spread. *Virology Journal* **2**:69 DOI [10.1186/1743-422X-2-69](https://doi.org/10.1186/1743-422X-2-69).
- Wang S, Witek J, Landrum GA, Riniker S. 2020b.** Improving conformer generation for small rings and macrocycles based on distance geometry and experimental torsional-angle preferences. *Journal of Chemical Information and Modeling* **60**:2044–2058 DOI [10.1021/acs.jcim.0c00025](https://doi.org/10.1021/acs.jcim.0c00025).
- Wang Y, Hu J, Lai J, Li Y, Jin H, Zhang L, Zhang L-R, Liu Z-M. 2020a.** TF3P: three-dimensional force fields fingerprint learned by deep capsular network. *Journal of Chemical Information and Modeling* **60**:2754–2765 DOI [10.1021/acs.jcim.0c00005](https://doi.org/10.1021/acs.jcim.0c00005).
- Wójcikowski M, Kukiela M, Stepniewska-Dziubinska MM, Siedlecki P. 2019.** Development of a protein-ligand extended connectivity (PLEC) fingerprint and its application for binding affinity predictions. *Bioinformatics* **35**:1334–1341 DOI [10.1093/bioinformatics/bty757](https://doi.org/10.1093/bioinformatics/bty757).
- Wójcikowski M, Zielenkiewicz P, Siedlecki P. 2015.** Open Drug Discovery Toolkit (ODDT): a new open-source player in the drug discovery field. *Journal of Cheminformatics* **7**:26 DOI [10.1186/s13321-015-0078-2](https://doi.org/10.1186/s13321-015-0078-2).
- Zeyrek CT, Arpacı ÖT, Arısoy M, Onurdağ FK. 2021.** Synthesis, antimicrobial activity, density functional modelling and molecular docking with COVID-19 main protease studies of benzoxazole derivative: 2-(p-chloro-benzyl)-5-[3-(4-ethyl-1-piperazynl) propionamido]-benzoxazole. *Journal of Molecular Structure* **1237**:130413 DOI [10.1016/j.molstruc.2021.130413](https://doi.org/10.1016/j.molstruc.2021.130413).
- Zhou L, Huntington K, Zhang S, Carlsen L, So E-Y, Parker C, Sahin I, Safran H, Kamle S, Lee C-M, Lee CG, Elias JA, Campbell KS, Naik MT, Atwood WJ, Youssef E, Pachter JA, Navaraj A, Seyhan AA, Liang O, El-Deiry WS. 2020.** MEK inhibitors reduce cellular expression of ACE2, pERK, pRb while stimulating NK-mediated cytotoxicity and attenuating inflammatory cytokines relevant to SARS-CoV-2 infection. *Oncotarget* **11**:4201 DOI [10.18632/oncotarget.27799](https://doi.org/10.18632/oncotarget.27799).